Analytical Analysis and Modeling of LFC-Heffron-Philips model for Optimized Hybrid Power System to enhance Power System Stability

Dr. V. S. Vakula[1], B. Rajesh[2]
[1]Assistant Professor, HOD, Dept. of EEE
[2]PG Scholar, Dept. of EEE
[1, 2] Jawaharlal Nehru Technological University, Kakinada University College of Engineering, Vizianagaram Campus.

Abstract **- The large deviation in wind speed and irregular solar radiation causes extreme fluctuations of output power in offshore wind farms and photovoltaic system respectively. In this perspective to minimize the deviation in frequency and bus voltages, One of the most simple and suitable options is to interconnect a DGS with conventional generation resources in the power system, However, in such hybrid Power systems (HPS), changes in the load demand and wind power variation disturb the frequency and bus voltages. This paper purposes for the integration of different distributed energy resources (DER) like offshore wind, stand-alone PV system, Industrial diesel engine generator ($IDEG$), Polymer electrolyte membrane fuel cells ($PEMFC$) with energy storage elements like battery energy storage system ($BESS$), flywheel energy storage system ($FESS$), ultracapacitor (UC), along with LFC-Heffron-Philips model (HPM) as conventional generation resources. All the models are simulated using MATLAB/SIMULINK, a relative and graphical assessment of frequency deviation and bus voltages for different hybrid power systems is also carried out in the presence of high-voltage alternating current ($HVAC$) line and high-voltage direct current ($HVDC$) link. Thus further aims for Analytical analysis and modeling of optimized hybrid power system to enhance power system stability. Analytical analysis reflects the enhancements in frequency and bus voltages deviation profiles with use of LFC-Heffron Philips model of a single-machine infinite bus ($SMIB$) system, also graphical and quantitative analysis of square integral error ($S.I.E$).**

Index Terms **-** *Hybrid Power System, Heffron-Philips model, Load frequency control, Frequency deviation, Energy storage systems, Power system stability, Power system damping, Proportional Integral controller (PI).*

I. INTRODUCTION

In electrical power industry, energy sources are broadly classified into two types, conventional and non-conventional sources. From earlier days the world is dependent on conventional energy sources mostly but if it remains at some point their survival may be terminated. Majority sources of energy are Conventional energy sources whereas non-conventional sources produce energy in insignificant amounts, so the future demands can't be met with only non-conventional sources. Hence, there is a need to protect the conventional energy sources for the future drive. In present days the focus is on the better utilization of non-conventional energy source along with conventional energy a source due to above-mentioned reasons [1-5]. This combined process of conventional and non-conventional energy sources is known as hybrid power system [1-5].

A power system is the interconnection of loads and generators in the real time. Effective operation of a power system is to be subject to provide reliable and uninterrupted power service to the loads. Default the loads must be fed at constant frequency and voltage at all the times. In the practical terms, this means that both voltage and frequency must be held within tolerable limits and power oscillations to be minimized to some extent. The process of maintaining frequency within limits is known as load frequency control of power system.

However, in such hybrid Power systems, changes in the load demand and wind power variation disturb the frequency and bus voltages. These purposes for the integration of different distributed generation systems like offshore wind, stand-alone PV system, Industrial diesel engine generator, Polymer electrolyte membrane fuel cells with energy storage elements like BESS and FESS, UC, along with LFC-Heffron-Philips model[1-2] as a conventional generation resource. A relative and graphical assessment of frequency deviation and bus voltages for different hybrid power systems is also carried out in the presence of HVAC line and HVDC link. Thus further aims for Analytical analysis and modeling of optimized hybrid power systems to enhance power system stability. The analytical analysis reflects the enhancements in frequency and bus voltages deviation profiles with use of LFC-Heffron Philips model of a SMIB[4] system. The rest of this paper is organized as follows: Section 2.describes the simplified system modeling with proposed LFC-Heffron Philips model [6]. Modeling of hybrid power system with energy systems in section 3. Configuration of the proposed system in section 4. Results, discussions and graphical analysis of square integral error (S.I.E) are presented in section 5. With finally some Conclusions are presented in section 6.

II. SYSTEM MODELLING

Mathematical modeling of each resource in distributed generation which is present in system under study is discussed. As shown in Fig. 1. Represents the system block diagram of hybrid power system.

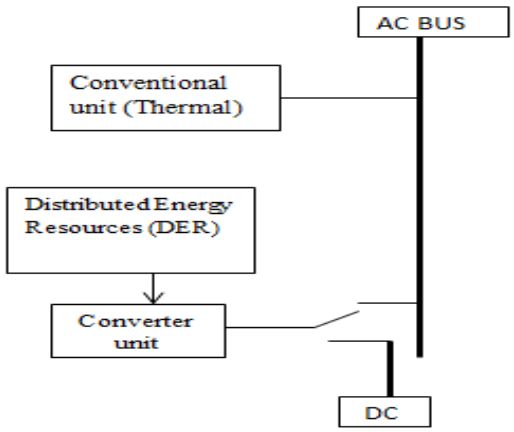

Fig. 2.1. System block diagram

2.1 MODELLING OF LOAD FREQUENCY CONTROL

Load frequency control unit scheme consists of three important parts:

- Turbine speed governing system
- Turbine
- Generator and Load

Here generator model is taken as Heffron-Philips model.

2.1.1 *Model of speed governing system:*

Assume the system is initially operating under steady-state conditions. It means that the linkage mechanism stationary and pilot valve closed and the steam valve opened definite magnitude, turbine running at constant speed with turbine output balancing the generator load. Let the operating conditions be characterized by

fo = System frequency

P_g = Generator input = turbine output (neglecting losses).

ΔY = change in Steam valve setting.

ΔP_C is the command of change in power.

For simplicity final mathematical relation of speed governing system can write as

$$\Delta Y(s) = \left[\Delta P_C(s) - \frac{1}{R}\Delta F(s)\right]\left[\frac{K_{Sg}}{(1+STsg)}\right] \quad (1)$$

Where, $R = \frac{K1KC}{K2}$ = governor speed regulation.

$Ksg = \frac{K1KCK3}{K2}$ = speed governor gain.

$Tsg = \frac{1}{K4K5}$ = speed governor time constant.

Equation (1) is represented in the form of a block diagram in Fig. 2.2.

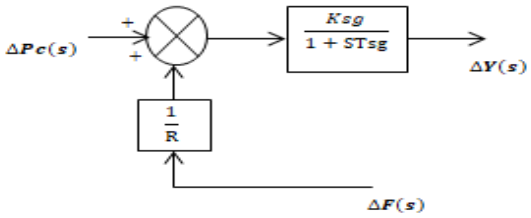

Fig. 2.2. Speed governor block diagram

2.1.2 *Turbine Model*

The dynamic response of a steam turbine in terms of deviation in power output to change in steam valve opening Y. Fig. 2.3 shows a two stage steam turbine with a reheat unit.

The dynamic response is largely affected by two factors:

1) Entrained steam between the inlet steam valve and first stage of turbine.

2) The storage action in the reheater, which causes the output of low pressure stage to lag behind that of the high pressure stage.

Thus, the turbine transfer function is characterized by two time constants. For ease of analysis, it will be assumed here that turbine can be modelled to have a single equivalent time constant. Fig 2.4 and 2.5 shows the transfer function model of a steam turbine without reheat and with reheat unit respectively. Typically the time constant T1 lies in the range 0.2–2.6 s.

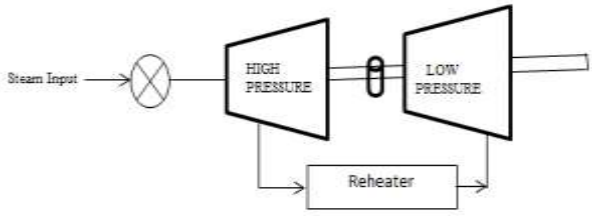

Fig. 2.3. Dual Stage Steam Turbine

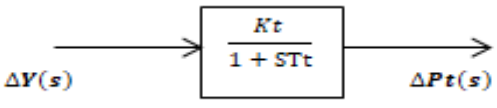

Fig 2.4. Turbine Transfer Function

Fig. 2.5. Turbine with Reheat unit

2.1.3 *Generator Load model*

Here generator load model is taken as Heffron-Philips model with AVR+PSS [3]. LFC-Heffron-Philips model is shown in Fig. 2.6 and Fig. 2.7.

Mechanical equations:

$$\delta^{\cdot} = \omega o \Delta\omega. \quad (2)$$

$$\Delta\omega^{\cdot} = \frac{1}{2H}\left(P_m - P_g\right) - \frac{D}{2H}\Delta\omega. \quad (3)$$

Generator Electrical dynamics:

$$Eq^{'} = (E_{fd} - E_q)/T_{do}^{'}. \quad (4)$$

Electrical equations:

$$P_g = E_q^{'} i_{tq} + \left(X_q - X_d^{'}\right) i_{td} i_{tq}. \quad (5)$$

$$E_q = E_q^{'} + \left(X_q - X_d^{'}\right) i_{td}. \quad (6)$$

$$V_{\vec{t}} = \sqrt{\left(E_q^{'} - X_d^{'} i_{td}\right)^2 + \left(X_q i_{tq}\right)^2} \quad (7)$$

Increment in power input to the generator load system

$$\Delta P_G - \Delta P_D$$

ΔP_G - Incremental turbine power output.
ΔP_D - The load increment.

Rate of stored kinetic energy in the generator rotor. At scheduled frequency (f), the stored energy is

$\omega o K_E = H * Pr$ KW- s (kilo joules).

Where Pr is the kW rating of the turbo-generator and H is defined as its inertia is constant. The kinetic energy being proportional to square of speed (frequency).

Final power balance equation we have

$$\Delta P_G - \Delta P_D = \frac{2HPr}{fo}\frac{d}{dt}\Delta f + B\Delta f \quad (8)$$

By rearranging and applying Laplace transform to the above equation, we get $\Delta F(s)$

$$= \left[\left(\Delta P_G(s) - \Delta P_D(s)\right) \Big/ \left(B + (2H/f_S)\right)\right]$$

$$= \left[\Delta P_G(s) - \Delta P_D(s)\right] T_H(s)$$

Linearized transfer function of Heffron-Philips model for Fig.2.7 is:

$T_H(s)$ = [12.4 s^5 + 536.5 s^4 + 3791 s^3 + 8112 s^2 + 6073 s + 1068

---

s^7 + 43.26 s^6 + 308.7 s^5 + 1010 s^4 + 2140 s^3 + 3651 s^2 + 2798 s + 501.9].

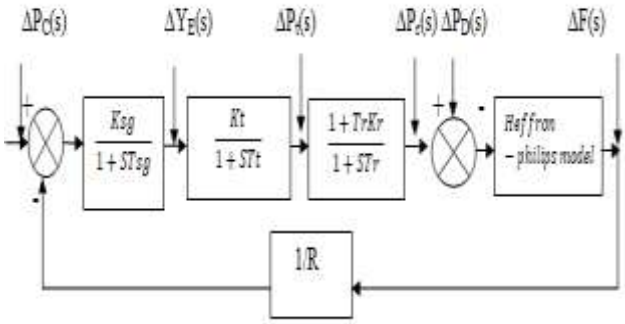

Fig. 2.6. LFC-Heffron-Philips model

The Parameters of the Heffron-Philips model of the SMIB system is from Appendix A.

Where $K1, K2, K3, K4, K5, K6$ are from Appendix B. and $K1, K2, K3, K4, K6$ are usually positive [2].Linearizing state (2)-(7), the full state linearized model of studied generator model is obtained as [3].

$$\begin{bmatrix} \Delta\delta. \\ \Delta w. \\ \Delta Eq'. \end{bmatrix} = \begin{bmatrix} 0 & wo & 0 \\ -\frac{k1}{M} & -\frac{D}{M} & -\frac{k2}{m} \\ -\frac{k4}{Tdo'} & 0 & -1/Tdo'k3 \end{bmatrix} \begin{bmatrix} \Delta\delta \\ \Delta w \\ \Delta Eq' \end{bmatrix} + \begin{bmatrix} 0 \\ 0 \\ \Delta Tdo'. \end{bmatrix} [\Delta Efd] \quad (9)$$

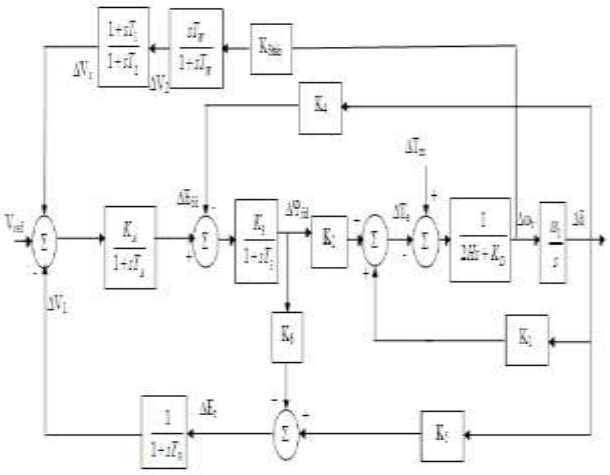

Fig. 2.7. Heffron-Philips-model with AVR+PSS

2.2 wind power generation

2.2.1. Modeling of wind speed in large band

Van der hoven model [20] is considered as a reference model for designing the wind speed in this hybrid distributed energy resource system (DER)

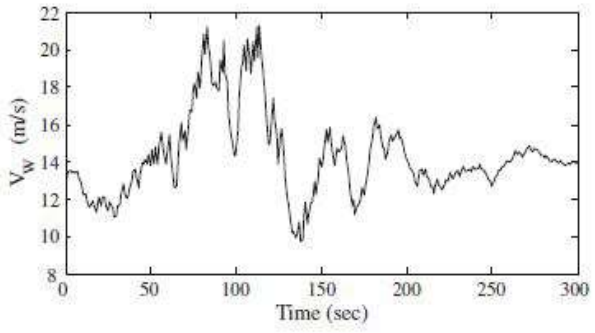

Fig. 2.8 system response for van der hoven model of large band wind speed over a period of 300s.

In van der hoven model the power spectrum of the horizontal wind speed is calculated in a range from 0.0007to 900 cycles/h. As shown in Fig.2.8 wide frequency range consists of medium and long term fluctuations.

2.2.2. Wind power

The power generated from the wind turbine generator (WTG) depends upon the wind speed (V_W).The wind speed is considered to be the total summation of the base wind speed (V_{WB}), ramp wind speed (V_{WR}), gust wind speed (V_{WG}), and noise wind speed (V_{WN}).by this wind speed is given by the following equation:

$$V_W = V_{WB} + V_{WR} + V_{WG} + V_{WN} \quad (10)$$

The mechanical power output of the wind turbine expresses as the

$$P_{WP} = (1/2)\, \rho\, A_R\, C_P\, V_W{}^3 \quad (11)$$

$\boldsymbol{\rho}$ - Is the air density (kg/m^3), A_R- is the swept area of the blade (m^2) and C_P - is the power co-efficient which is a fraction of tip speed ratio ($\boldsymbol{\lambda}$) and blade pitch angle ($\boldsymbol{\beta}$).

The transfer function of wind turbine generator is given by a simple linear first order lag by neglecting all the non-linearity's.

$$G_{WTG}(s) = \frac{\Delta Pwtg}{\Delta Pwp} = \frac{Kwtg}{(1+STwtg)} \quad (12)$$

Where $\boldsymbol{K_{WTG}}$ is the gain constant and $\boldsymbol{T_{WTG}}$ is the time constants.

2.3 Photovoltaic (stand-alonePV) power generation

PV System consists of many cells connected in series and parallel to provide the desired voltage and current .the voltage and current bond is non-linear by default. The maximum power output of the PV array varies according to the solar radiation or load current which is changing all the time .Therefore control strategy is required to use solar radiation most effectively in order to attain maximum power.

The output of the PV system module can be expressed as the following equation:

$$P_{PVPG} = \eta S \emptyset [1 - 0.05(T_a + 24)] \quad (13)$$

Where η- is the conversion efficiency of the PV array, S - the surface measured area of the PV array (m^2), $\emptyset$ - is the solar radiation (Kw/m^2) and Ta-is the ambient temperature in (^{o}C) .The transfer function of PV is in the simple linear first order lag is given as:

$$G_{PV}(s) = \frac{\Delta P_{PVPG}}{\Delta \emptyset} = \frac{K_{PV}}{(1+ST_{PV})} \quad (14)$$

Where $\boldsymbol{K_{PV}}$ is the gain constant and $\boldsymbol{T_{PV}}$ is the time constants.

2.4 Polymer electrolyte membrane fuel cells ($PEMFC$) power generation

Unlike conventional fuel cells, polymer electrolyte membrance fuel cell [10] ($PEMFC$) offers great advantages over it. This cells are static energy conversion devices which converts the chemical energy of fuel i.e. hydrogen ,directly into electrical energy .They are considered to be an important resource in hybrid distributed energy resources due to advantages like high efficiency ,low pollution etc. Non consideration of all the non-linearities, transfer function of $PEMFC$ can be given by first order lag as given:

$$G_{PEMFC}(s) = \Delta P_{PEMFC}/\Delta f = K_{PEMFC}/1+ST_{PEMFC} \quad (15)$$

Where $\boldsymbol{K_{PEMFC}}$ is the gain constant and $\boldsymbol{T_{PEMFC}}$ is the time constants.

2.5 Industrial diesel engine power generation ($IDEG$)

Industrial diesel engine generator ($IDEG$) works autonomously to supply the deficit power to the hybrid power system to meet the required supply-load demand balance condition.

The transfer function of $IDEG$ can be given by a first order lag as:

$$G_{IDEG}(s) = \Delta P_{IDEG}/\Delta f = K_{IDEG}/1+ST_{IDEG} \quad (16)$$

2.6 Aqua-electrolyzer (AE) for production of hydrogen

A part of P_{WPG} and P_{PV} is to be utilized by Aqua-electrolyzer for the production of the hydrogen to be used in PEMFC for generation of power.

Its first order transfer function can be written as:

$$G_{AE}(s) = K_{AE}/1+ST_{AE} \quad (17)$$

Where K_{AE} is the gain constant and T_{AE} is the time constants.

2.7 BESS/FESS as energy storage system

Battery energy storage system ($BESS$) is mainly used for load leveling, harmonic distortion cancellation and bus voltage control. It could also be utilized to provide some additional damping to first order hybrid power system swings to improve both transient and dynamic stability .It can provide rapid change of active and reactive power both in positive and negative value .It is modulated to oppose any frequency [7] oscillation in the hybrid power system.

$G_{BESS}(s) = \Delta P_{BESS}/\Delta f = K_{BESS}/1+ST_{BESS}$ (18)

Where K_{BESS} is the gain constant and T_{BESS} is the time constants.

Where Flywheel energy storage system ($FESS$) or Electromechincal battery. It is kinetic energy storage device behaves like batteries.

Transfer function of the $FESS$ can be represented as first order lag given as:

$G_{FESS}(s) = \Delta P_{FESS}/\Delta f = K_{FESS}/1+ST_{FESS}$ (19)

Where K_{FESS} is the gain constant and T_{FESS} is the time constants.

2.8 Ultra capacitors as alternative storage devices

Ultracapacitor (UC) is the electromechanical type capacitors .It has fast charging-discharging capability, longer life, almost no maintenance and environmental friendliness. UC Is used to store electrical energy during surplus generation and deliver high power within a short duration of time during peak-load demand [22].

Transfer function of the UC can be represented as first order lag given as:

$G_{UC}(s) = \Delta P_{UC}/\Delta f = K_{UC}/1+ST_{UC}$ (20)

Where K_{UC} is the gain constant and T_{UC} is the time constants.

2.9. PI CONTROLLER

Proportional-integral (PI) controllers [6] are used before $PEMFC$,$IDEG$, AE to minimize the mismatch in supply and power demand. Hence the frequency deviation in presence of storage system combinations of hybrid power systems.

Transfer function of the conventional PI controller can be given as:

$G_{PI}(S) = K_P(1+1/Tis)$ (21)

K_P is the proportional gain constant and Ti is the integral gain.

The input of each controller installed before $PEMFC$, $IDEG$, and AE is the error (ΔP_e) in supply demand .And the product of the frequency deviation of the power system and gain($K\Delta f$). Frequency deviation (Δf) is very small as compared to deviation in the supply (ΔP) due to high gain product. On the basis of trail-and-error method [23] gain constant values are taken. Then the supply error (ΔP_e) and frequency deviation (Δf) is very small .values of the gain constant of aqua-electrolyzer (K_{AE}), $PEMFC$ (K_{PEMFC}), industrial diesel engine generator (K_{IDEG}) are taken as $50,10,40$ respectively.

III. CONFIGURATION OF DISTRIBUTED ENERGY RESOURCES (DER) AND STORAGE SYSTEMS

Different combinations of hybrid energy resources [1] are integrated to form hybrid power system as shown in Fig. 3. Mainly in this analysis power is generated through the three energy sources WTG,PV, $PEMFC$, $IDEG$ and AE as shown to be converted a part of generated power from PV or WTG for hydrogen production to be used by Polymer electrolyte membrane fuel cell.

The total output power of the hybrid DG system is expressed by [1, 5]

$$\Delta P_{DGS} = \Delta P_{WP+} \Delta P_{FC} + \Delta P_{AE} + \Delta P_{DEG} \pm \Delta P_{BESS} \quad (22)$$

Power balance is attained by the following equation [1, 4]

$$\Delta P_e = \Delta P_{TH+} \Delta P_{DGS} - \Delta P_D \quad (23)$$

Change in frequency profile (Δf) can be expressed as

$\Delta f = \Delta Pe/Ksys$ (24)

Where Ksys is the system characteristic constant of hybrid power system.

Transfer function of system variation to per unit change can be expressed as:

$G_{SYS} = \Delta f / \Delta Pe = 1/Ksys(1+STsys) = 1/D+Ms$ (25)

Where D = damping constant and M = inertia constant of hybrid power system [16]

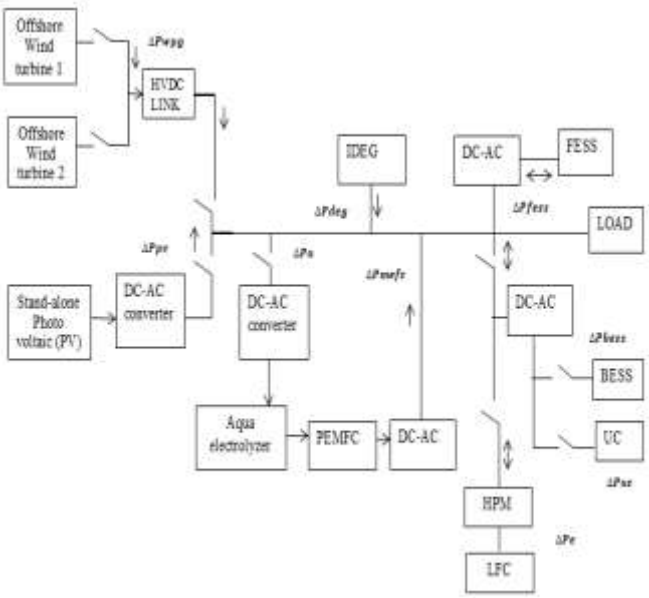

Fig. 3. Configuration of hybrid energy and storage systems

IV. INTEGRATION TOPOLOGIES FOR ISOLATED HYBRID POWER SYSTEMS

Distributed generation (DG) the different energy resources [24] need to be connected to form hybrid power system for security reasons. In this analysis mainly three integration topologies along with other energy storage systems and with Heffron-philips model is shown in Fig. 4.Three hybrid power systems consists of power generating sources as offshore $WTGs$, Stand-alone ,PV, $PEMFC$, and $IDEG$ with energy storage system combinations are $BESS-FESS$.Power converters are used for properly operated for the power balance condition.

4.1. Hybrid power system (HPS-1)

In this case consider two offshore WTGs connected to generate wind power P_{WPG} in the system. HVDC link is considered to transmit the wind power generation; the DC power (P_{HVDC}) output is converted to AC power by preferred converter and is fed to the AC load indirectly and directly to the DC load. The total wind power generation P_{WPG} or P_{HVDC} is utilized in the aqua-electrolyzer to produce hydrogen as a fuel for the PEMFC. The PEMFC generates DC power which is converted to AC by suitable converter. P_{PEMFC} is combined with IDEG output P_{IDEG} and P_{WPG} or by P_{HVDC} for the power supply to the connected loads. The surplus power of the considered hybrid power system is conveniently stored in BESS-FESS or UC-FESS through suitable power converters.

Thus the resultant power generation can be shown as:

$$\Delta P_H = \Delta P_{WP} + \Delta P_{PEMFC} - \Delta P_{AE} + \Delta P_{IDEG} \pm \Delta P_{BESS} \pm \Delta P_{FESS} \quad (26)$$

Table 1.Componets of Hybrid power system

Topology	Distributed energy resources(DER) or Storage elements
HPS-1	2-WTGs+1-AE+1-PEMFC+1-IDEG+1-BESS+1-FESS/UC
HPS-2	2-WTGs+1-IDEG+1-BESS+1-FESS/UC
HPS-3	2-WTGs+1-AE+1-PEMFC+1-IDEG+1-PV+1-BESS+1-FESS/UC

4.2. Hybrid power system (HPS-2)

In this hybrid power system first consider two offshore WTGs connected to the system while AE and PEMFC are removed from the system. The surplus power of the analyzed hybrid power system is stored in BESS/UC and FESS. The total absorbed by the connected load can be expressed by

$$\Delta P_H = \Delta P_{WP} + \Delta P_{IDEG} \pm \Delta P_{BESS} \pm (\Delta P_{FESS} \text{ or } P_{UC}) \quad (27)$$

4.3. Hybrid power system (HPS-3)

In this hybrid power system first, consider two offshore WTGs and PV connected to the system while AE and PEMFC are remained connected. As in the equation(28), the total power generation by offshore wind is combined with a power output of stand-alone PV system i.e. PPVPG The surplus power of the analyzed hybrid power system is stored in BESS/UC and FESS. In this analysis resultant power generation is more due to all energy resources the total power absorbed by the connected load can be expressed by

$$\Delta P_H = \Delta P_{WP+} \Delta P_{PVPG} + \Delta P_{PEMFC} - \Delta P_{AE} + \Delta P_{IDEG} \pm \Delta P_{BESS} \pm \Delta P_{FESS} \quad (28)$$

Different combinations of hybrid power systems as shown in Fig.4 combined to have a reliable and continuous power supply to end users. As renewable energy system can be used as a stand-alone power system for providing electricity in the remote areas. Thus minimization of frequency deviation (Δf) and bus voltage variation helps to build a robust system.

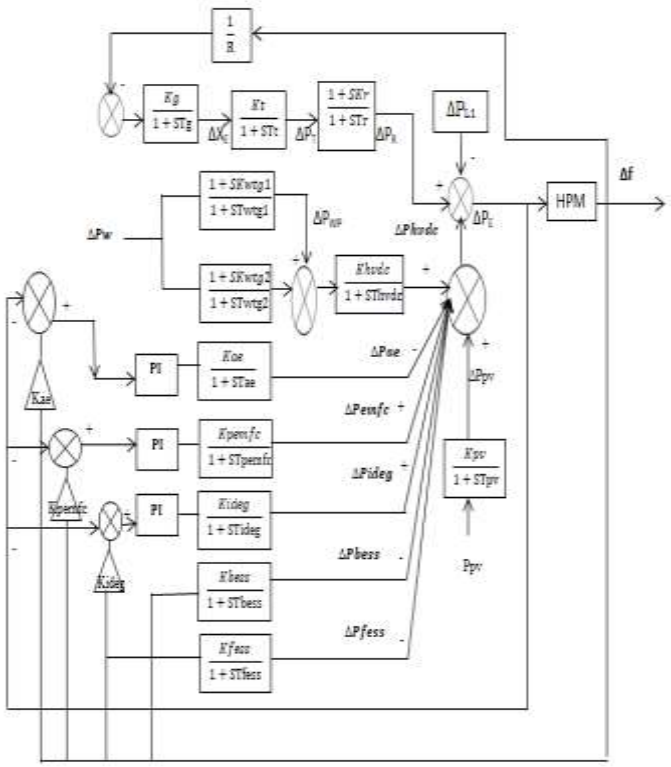

Fig. 4. Block diagram for hybrid power system with LFC-HPM

V. RESULTS AND DISCUSSIONS

5.1 Presence of damping coefficient due to HPM.

As shown by Fig. 5, the number of Power Oscillations of the Damping is close to one when damping coefficient is noticeable up to 0.459. As compared when damping coefficient is less than 0.159 [17], the generator active power oscillation is more than three when used Heffron-Philips model.

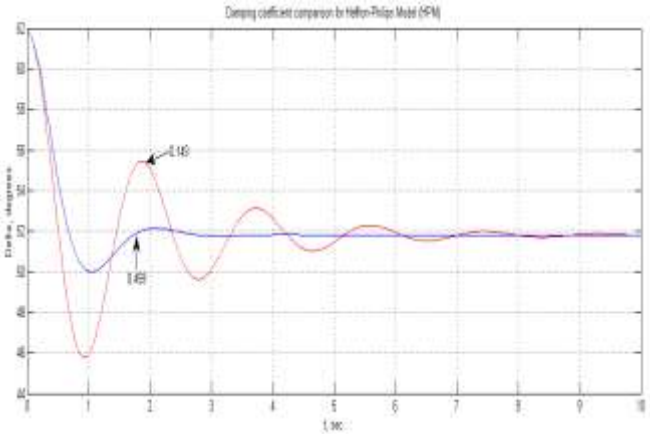

Fig. 5. Damping coefficient comparison when ξ<0.159 and ξ=0.459.

5.2 Deviation of terminal voltage and field voltages in HPM from HPS-1, HPS-2, and HPS-3 with PI controller in HVAC line.

It gives better profile in minimization of terminal voltage and field voltage deviation close to zero due to LFC-Heffron-Philips model even when photo-voltaic generation added in HPS-3. When storage elements added to the isolated hybrid power systems this proposed system is taken as a combination of HPM-BESS-FESS. (a) Shows deviation in terminal voltage is 0.01 in p.u. for HPS-1 and HPS-2 while in HPS-3 this deviation is close to zero gives efficient minimization of terminal voltage deviation. (b) On the other side deviation in the field voltage is -1.5 for HPS-1 and HPS-2 while in HPS-3 is -0.1 and this deviation is close to zero.

(a)

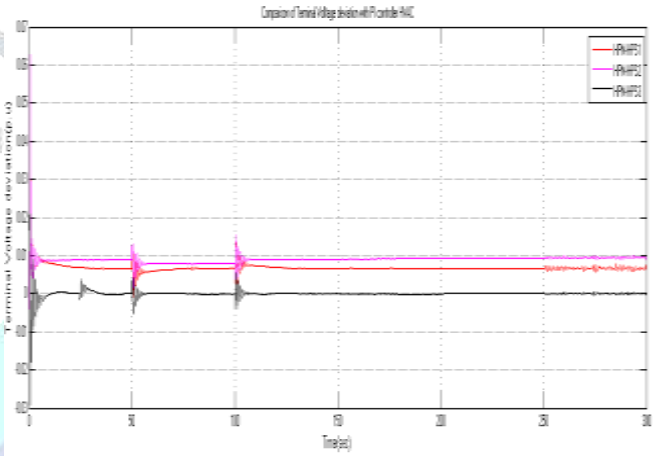

(b)

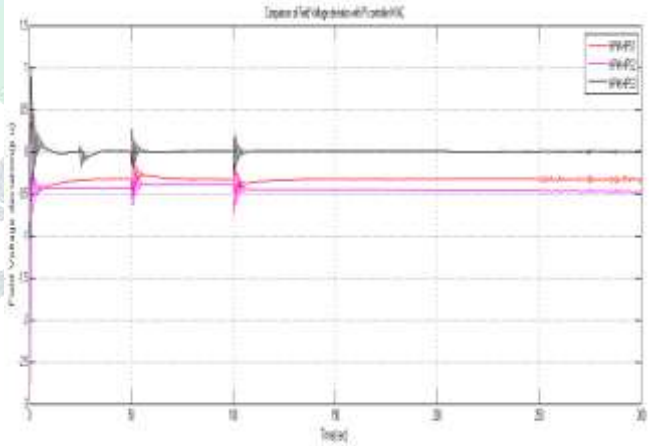

Fig. 6. System responses for ΔV_t (p.u.) & ΔE_{fd} (p.u.) 5% step change in terminal reference voltage.

5.3 HVAC LINE

5.3.1 HPS-1 with Different combinations with and without PI with HVAC line.

For every system, the load request is taken to be 1.0 p.u. diminished to 0.5 p.u. at t = 50s, stays same up to t = 100s and after that suddenly expanded again to 1.0 p.u. at t = 100 s, kept up steady till t = 300s. The breeze speed is

taken as 7.5 m/s amid $0 < t < 200$ s, all of a sudden diminished to 4.5 m/s at t = 200 s and stays consistent at a similar incentive till t = 250 s, abruptly expanded to 15m/s at t = 250 s and stay at a similar incentive till t = 300 s.

is shown in Fig.7.The load demand is assumed to constant at 1.0 p.u. for $0 < t < 50$ s, decreased suddenly at t=50 s and remain constant at 0.5 p.u. for $50 < t < 100$ s and increased suddenly to 1.0 p.u. at t=100 s and assumed constant at 1.0 p.u. for $100 < t < 300$ s.

For Fig.7. HPS-1 without PI Controller at NO BESS Δf = -0.8 for BESS-FESS Δf = -0.7 for UC-FESS Δf = -0.15 for HPM-BESS-FESS Δf = -0.05.

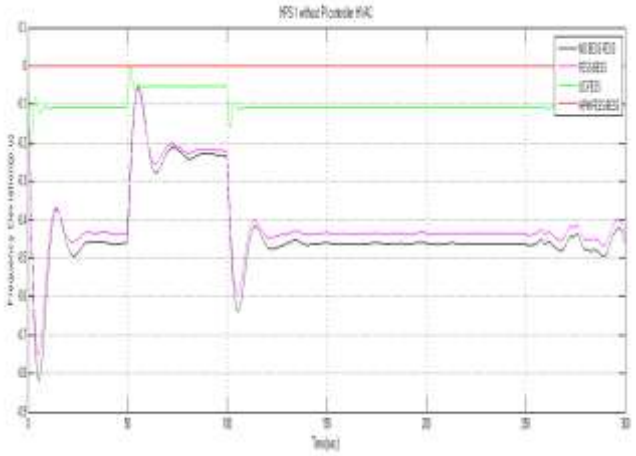

Fig. 7. Simulation results of HPS-1 without PI controller with HVAC line.

As shown in Fig.8 the deviations using connected Heffron-philips model is 30% less than the deviations using ultra-capacitor along with the some energy storage elements for a load change of 0.01.p.u.

For Fig.8. HPS-1 without PI Controller at NO BESS Δf = -0.8 for BESS-FESS Δf= -0.7 for UC-FESS Δf = -0.15 for HPM-BESS-FESS Δf = -0.05.

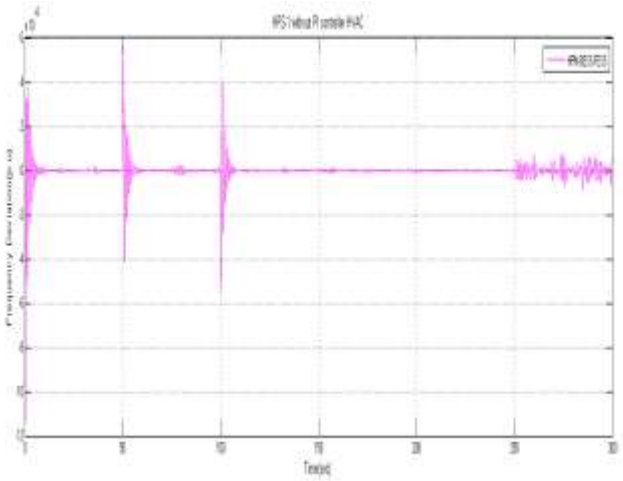

Fig. 8. Simulation results of HPS-1 without PI controller with HVAC line for HPM-BESS-FESS.

For Fig.9. HPS-1 without PI Controller at NO BESSΔf= -0.12 for BESS-FESS Δf = -0.1 for UC-FESS Δf = -0.01 for HPM-BESS-FESS Δf = -0.0011.

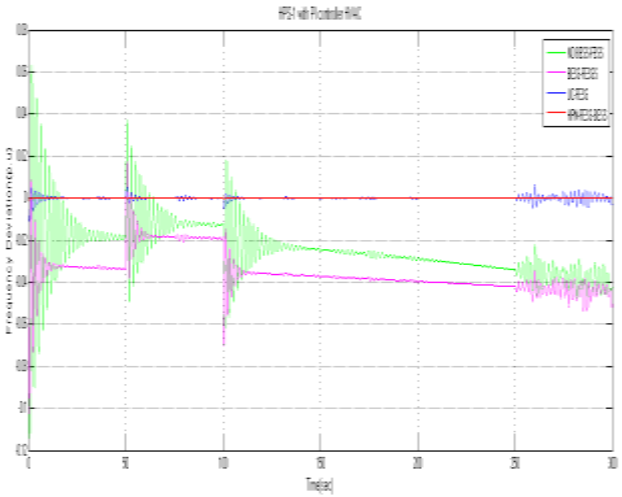

Fig 9. Simulation results of HPS-1 with PI controller with HVAC line.

As shown in Fig. 8. Minimization of Frequency deviation (Δf) using HPM-BESS-FESS gives better profile over a period of 100<t<300 s. with 1% step change in input to the LFC-HPM.

For Fig.10. HPS-1 without PI Controller at UC-FESS Δf = -0.01 for HPM-BESS-FESS Δf = -0.0011.

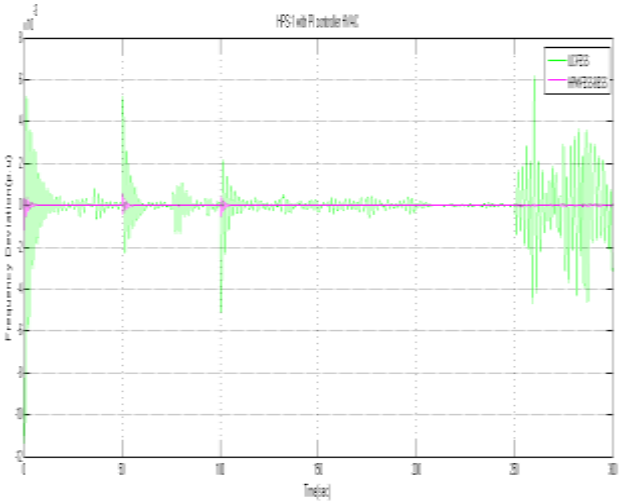

Fig. 10. Simulation results of HPS-1 with PI controller HPM-BESS-FESS with HVAC line.

For Fig.11. HPS-2 without PI Controller at NO BESS Δf = -0.6 for BESS-FESS Δf = -0.5 for UC-FESS Δf = -0.2 for HPM-BESS-FESS Δf = -0.0012.

HPS-2 with different combinations without PI controller is shown in Fig. 11. As Industrial diesel engine generator set (IDEG) is taken rather than the conventional type in this hybrid power system.

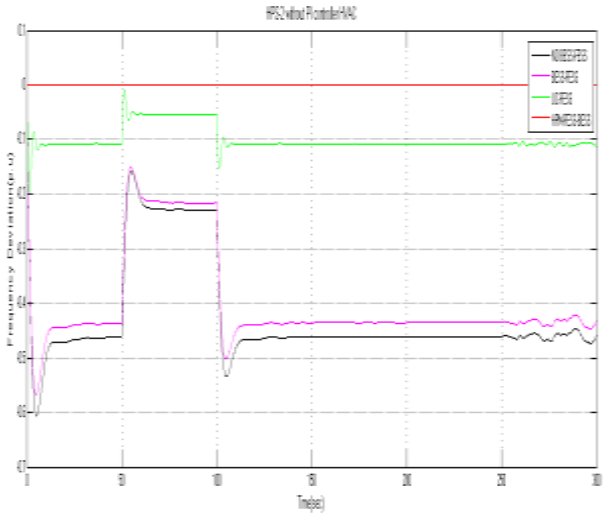

Fig. 11. Simulation results of HPS-2 without PI controller with HVAC line.

For Fig.12. HPS-1 without PI Controller at NO BESS Δf = -0.2 for BESS-FESS Δf = -0.15 for UC-FESS Δf = -0.05 for HPM-BESS-FESS Δf = -0.0011.

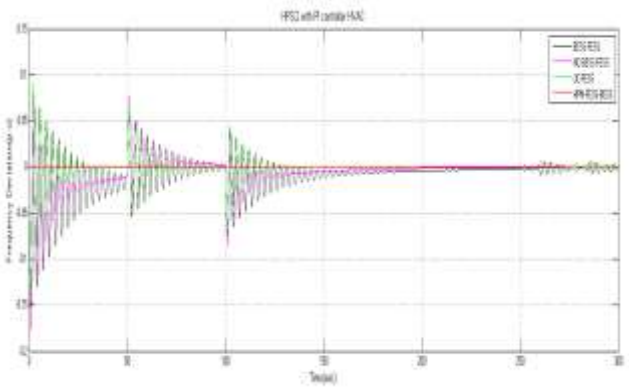

Fig. 12. Simulation results of HPS-2 with PI controller with HVAC line.

For Fig.13. HPS-1 without PI Controller at NO BESS Δf = 3 for BESS-FESS Δf = 2.5 for UC-FESS Δf = 0.5 for HPM-BESS-FESS Δf = 0.001.

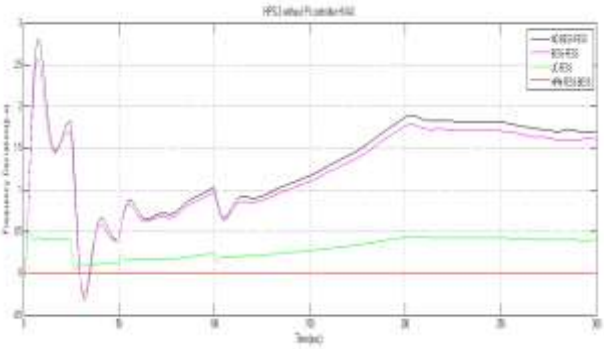

Fig. 13. Simulation results of HPS-3 without PI controller with HVAC line.

For Fig.14. HPS-1 without PI Controller at NO BESS Δf = 0.2 for BESS-FESS Δf = 0.15 for UC-FESS Δf = 0.05 for HPM-BESS-FESS Δf = 0.0015.

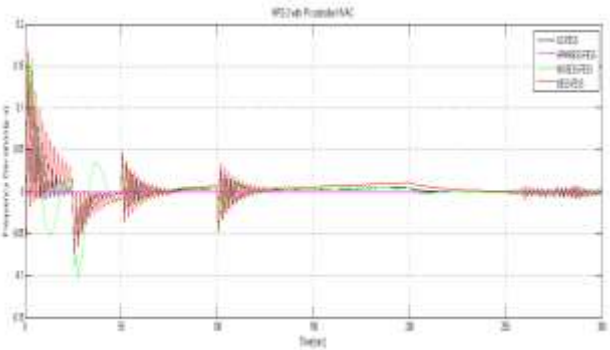

Fig. 14.Simulation results of HPS-3 with PI controller with HVAC line.

The load demand is met by conventional load frequency controlled (LFC) Heffron-Philips model (HPM), offshore dual wind turbine generators, Polymer electrolyte membrane fuel cells and the deficit power required is supplied by the industrial diesel engine generator. Aqua electrolyzer uses some portion of the dual wind turbine generator power output and produces hydrogen fuel for

PEMFC. The deviation in frequency of HPS-1 for different combinations of storage elements FESS-BESS, FESS-UC, and HPM-FESS-BESS and without storage elements is presented in Fig.7 to Fig.14.

In this three hybrid power systems sudden decrease and increase of load are applied at t=50 s and t=100 s the deviation in frequency is increasing suddenly at t=50 s and decreasing at t=100 s due to sudden mismatch in supply and load demand and get oscillates .After few seconds the frequency deviation is exhibiting less oscillation and comes back to the steady state by the proper tuning of PI controller. The comparative assessment clearly reflects that frequency deviation is less with use of Heffron-Philips model under PI controller action in comparison to other combinations.

5.4 HVDC LINK

5.4.1 HPS-1 with Different combinations with and without PI with HVDC link.

The same wind speed and load conditions are applied as presence in 5.3.Then deviation in frequency profiles are presented in Fig.15 to Fig 20. Due to sudden dissimilarity in wind speed and load, the frequency deviation profiles in three hybrid power systems[25] transmission losses are reduced and get less oscillates compare to HVAC link.

For Fig.15. HPS-1 without PI Controller at NO BESS Δf = -1.2 for BESS-FESS Δf = -0.7 for UC-FESS Δf = -0.1 for HPM-BESS-FESS Δf = -1.2E^{-3}.

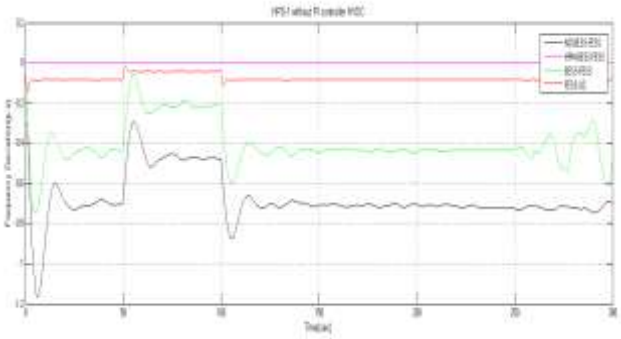

Fig. 15. Simulation results of HPS-1 without PI controller with HVDC link

For Fig.16. HPS-1 with PI Controller at NO BESS Δf = -0.15 for BESS-FESS Δf = -0.1 for UC-FESS Δf = -0.05 for HPM-BESS-FESS Δf = -1.1E^{-3}.

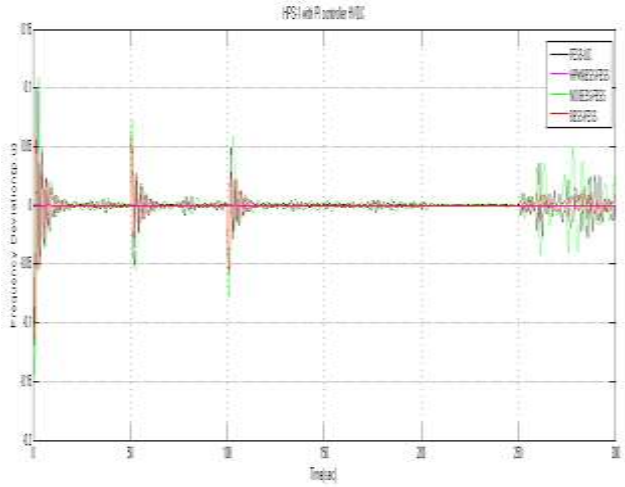

Fig. 16. Simulation results of HPS-1 with PI controller with HVDC line.

For Fig.17. HPS-2 without PI Controller at NO BESS Δf = -0.6 for BESS-FESS Δf = -0.5 for UC-FESS Δf = -0.2 for HPM-BESS-FESS Δf = -11E^{-4}.

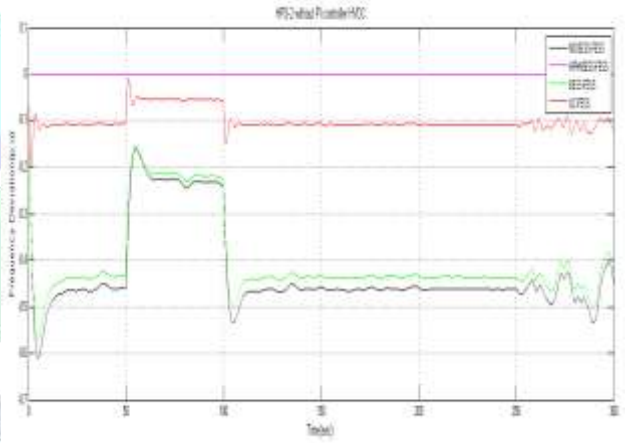

Fig. 17. Simulation results of HPS-2 without PI controller with HVDC line.

For Fig.18. HPS-2 with PI Controller at NO BESS Δf = -0.22 for BESS-FESS Δf = -0.19 for UC-FESS Δf = -0.1 for HPM-BESS-FESS Δf = -10E^{-4}.

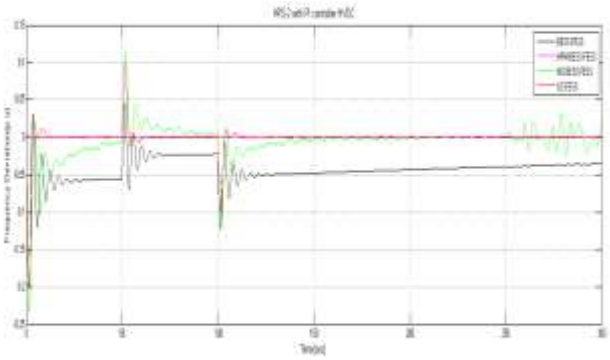

Fig. 18. Simulation results of HPS-2 with PI controller with HVDC line.

For Fig.19. HPS-3 without PI Controller at NO BESS Δf = -0.8 for BESS-FESS Δf = -0.7 for UC-FESS Δf = -0.2 for HPM-BESS-FESS Δf = -0.012.

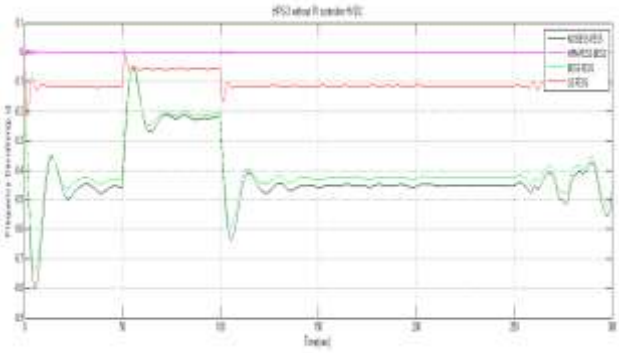

Fig. 19. Simulation results of HPS-3 without PI controller with HVDC link.

For Fig.20. HPS-3 with PI Controller for HPM-BESS-FESS Δf = -12E^{-4}.

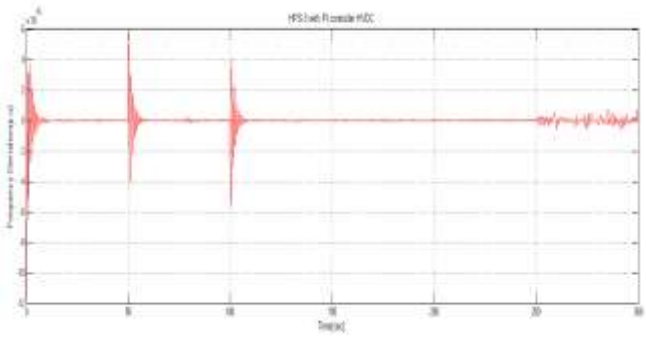

Fig. 20. HPS-3 with PI controller HVDC HPM-FESS-BESS

For Fig.21. HPS-3 with PI Controller at NO BESS Δf = -0.16 for BESS-FESS Δf = -0.11 for UC-FESS Δf = -0.07 for HPM-BESS-FESS Δf = -12E^{-4}.

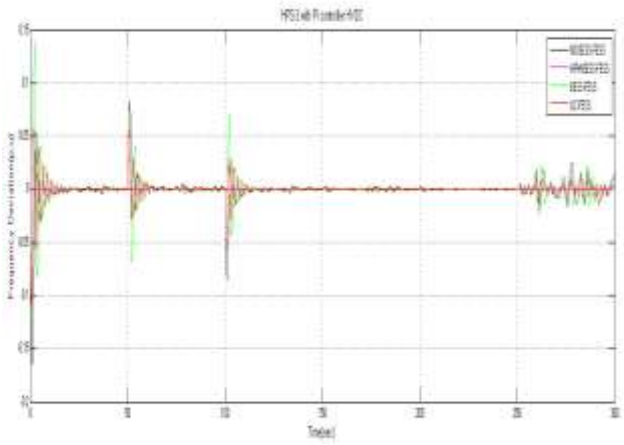

Fig. 21. Simulation results of HPS-3 with PI controller with HVDC link.

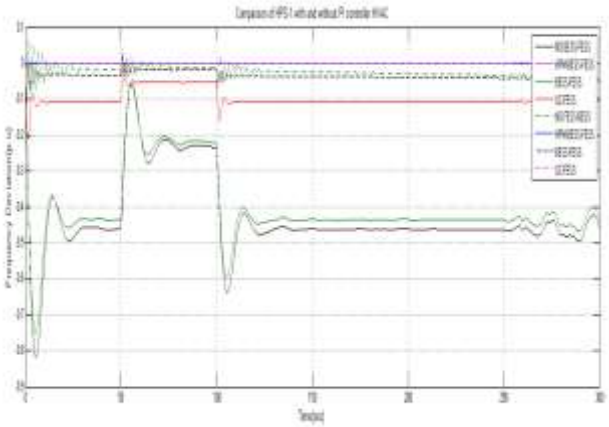

Fig. 22. Comparison of HPS-1 with and without PI controller with HVAC line.

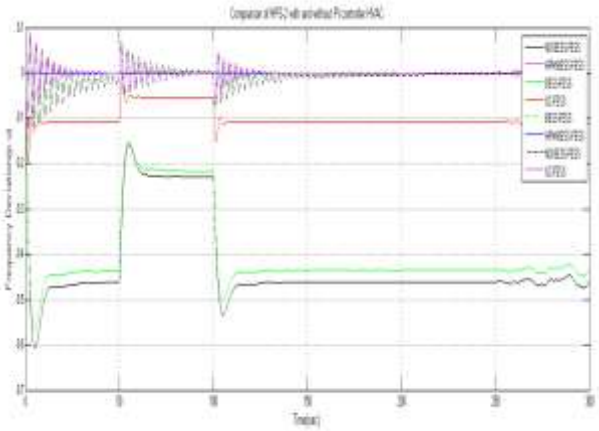

Fig. 23. Comparison of HPS-2 with and without PI controller with HVAC line.

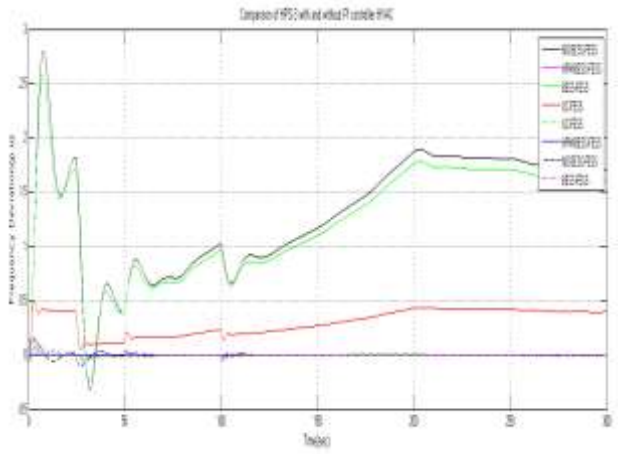

Fig. 24. Comparison of HPS-3 with and without PI controller 1983.with HVAC line.

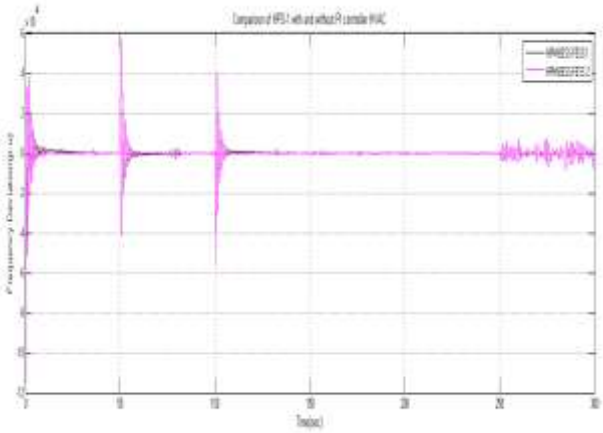

Fig. 25. HPS with and without PI controller HPM-BESS-FESS with HVAC line.

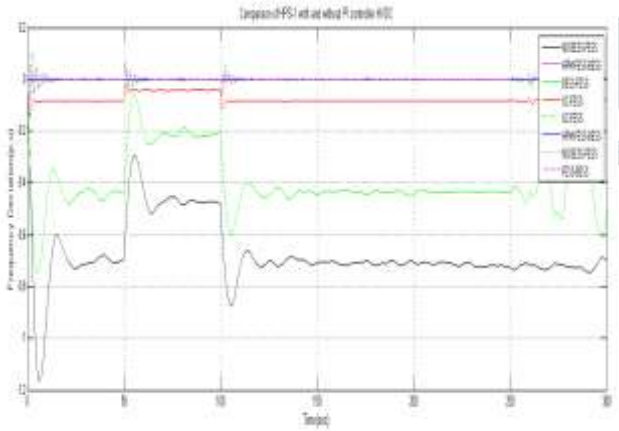

Fig. 26. Comparison of HPS-1 with and without PI controller with HVDC link.

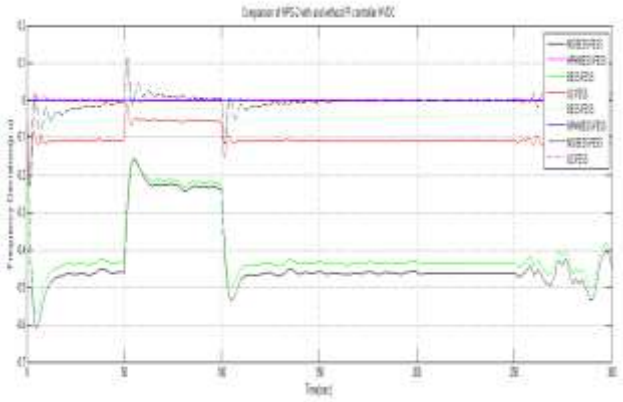

Fig. 27. Comparison of HPS-2 with and without PI controller with HVDC link.

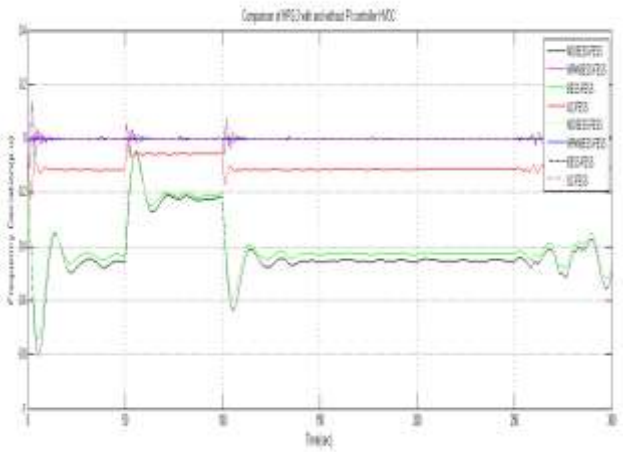

Fig. 28. Comparison of HPS-3 with and without PI controller with HVDC link.

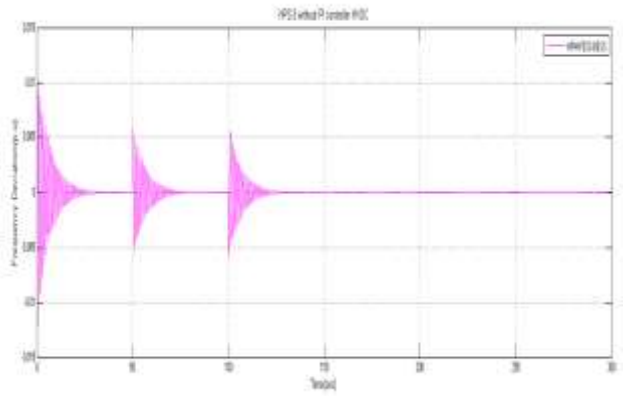

Fig. 29. HPS with and without PI controller HPM-BESS-FESS with HVDC link

Comparison of with and without PI controller for HPS-1, HPS-2 and HPS-3 with HVAC & HVDC is shown in Fig.22. to Fig.29.

The LFC-HPM is to improve the frequency deviation performance under 1% load disturbance conditions. In the proposed HPM-BESS-FESS, the AVR+PSS is used in Heffron-Philips model with high gain constants. They are

selected for the input load disturbance; it will influence the overshoot, stability, damping coefficient and steady state error of system responses. The HPM-BESS-FESS is provides minimum frequency deviation and less overshooting in presence of HVAC and HVDC link in hybrid power system. It is clearly determined that by using the HPM-BESS-FESS in hybrid distributed energy resources (DER), we have significant minimum frequency deviation as shown in Fig.22 to Fig.29.

5.6. GRAPHICAL ANALYSIS OF S.I.E

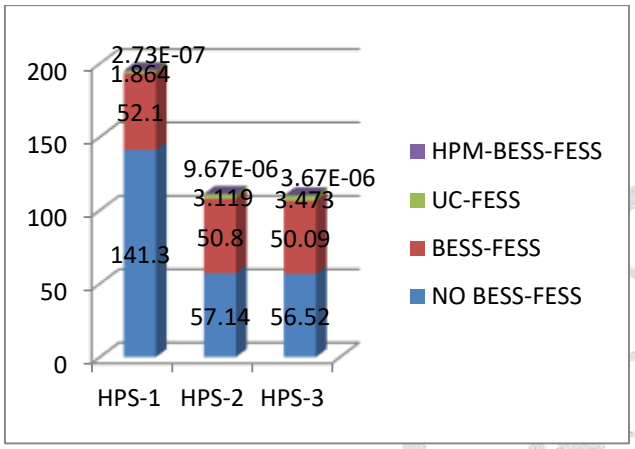

Fig 1. Graphical analysis of S.I.E without PI controller HVDC link

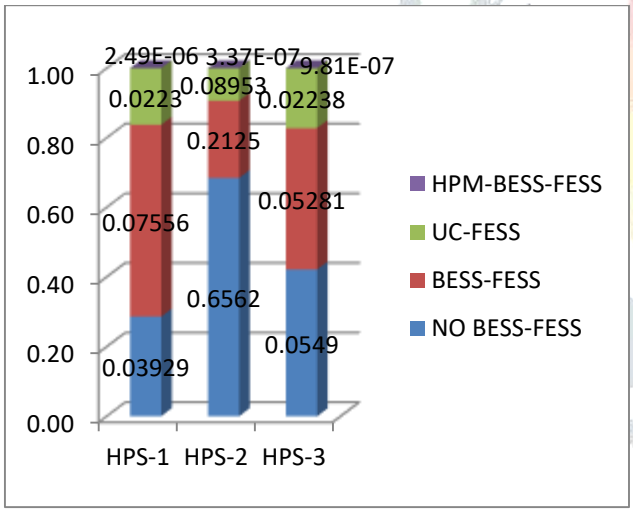

Fig 2. Graphical analysis of S.I.E with PI controller HVDC link

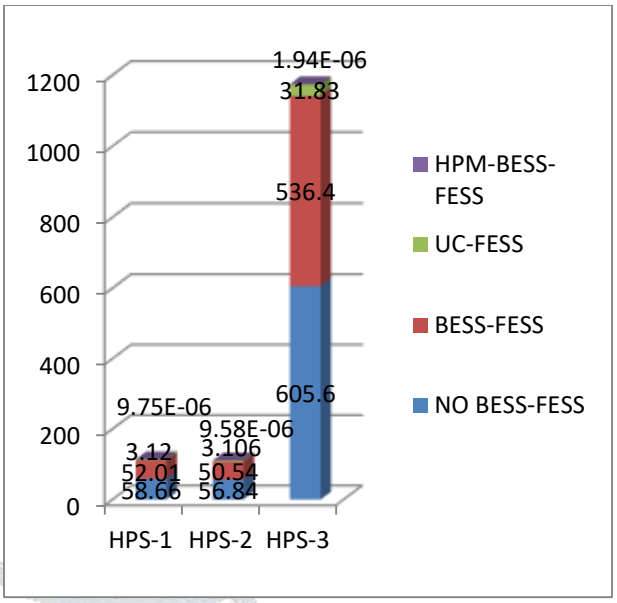

Fig 3. Graphical analysis of S.I.E without PI controller HVAC line

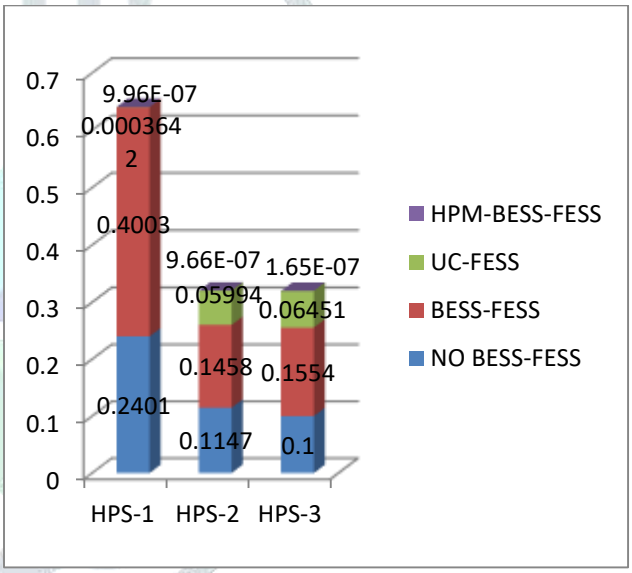

Fig 4. Graphical analysis of S.I.E with PI controller HVAC line

Quantitative data for this graphical analysis of square integral error from the frequency deviation for different hybrid power systems is presented in Appendix D. Table 1B.

VI. CONCLUSION

In this paper, the study of frequency deviation in isolated hybrid power systems with different combinations of energy storage elements is presented. The deviations in frequency profile for isolated hybrid power system[25] were studied, both qualitatively and quantitatively. Different combinations of the elements are considered and three combinations of the hybrid power systems are taken for analysis. The hybrid power system 2 does not contain Polymer electrolyte membrane fuel cell and aqua-electrolyzer but still can supply the load power with industrial diesel-engine generator. The hybrid power system 3 has large frequency

deviation when compared to the other two as it contains stand-alone photo-voltaic power generation which includes the fluctuations of solar radiation also. A relative assessment of frequency deviations with the storage combinations; $FESS - BESS$ $FESS$ –UC, HPM- $BESS$ - $FESS$ and with NO- $BESS$- $FESS$. A significant improvement in frequency deviation was observed from the simulation results with use of $FESS$ –UC as compared to $FESS - BESS$ and without storage cases.

A comparison in frequency deviation profile was presented for the hybrid power systems with both HVAC and HVDC link. The performance of the system is better with HVDC link when compared to that of HVAC link. Further comparison was carried out for different cases of hybrid power system combinations; with and without incorporation of PI controller and generator model is taken as LFC-Heffron Philips Model and the frequency deviations are also calculated in terms of square integral error (S.I.E) to validate the graphical results.

This work may be extended by fuzzy PID controller and executing various soft computing techniques for minimizing the frequency deviation, reducing peak overshooting further minimizing the steady state error of hybrid power distributed generation system under wind speed variation and load disturbance conditions.

The power quality and voltage stability of large power systems with biomass distributed energy resources (DER) with different FACTS device has to be studied. Voltage stability of power systems with a large share of distributed energy resources need to be studied further along with optimization of FACTS devices location. Battery charge controller can be designed for more reliable operation in a hybrid energy system. Neural networks can be applied in the systems to control the switching of solar and wind system individually. The SCADA device may be used to save the historical solar and Wind profile of any geographical place and analyses the electricity demand of that vicinity Based on these, proper load scheduling can be done.

Appendix A. The parameters of the Heffron-Philips model of SMIB system

K_1 = {EbEqoCos δo/(Xs+Xq)}+{EbIq0sinδ0(Xq-Xd')/(Xs+Xd')

K_2 = {iqo(Xs+Xq)/(Xs+Xd')}

K_3 = (Xe+Xd')/(Xs+Xd) (1.14)

K_4 = EbSinδ0(Xd-Xd)/(Xs+Xd')

K_5 = {(-XqVdoEbcosδ0)/((Xs+Xq)Vto)}

{Xd'VdoEbsinδ0/((Xs+Xd')Vto)}

K_6 = XsVqo/[((Xs+Xd')Vto)]

Appendix B. Parameters of example Hybrid Power System

Generator:

Xd=1.03; Xq= 0.6; Xd'=1; D= 0.39; Tdo'= 6s; H =7.6s; D =0.05. K_{SG} =1.0 ; T_{SG} =0.08 ;K_T = 1.0; T_T =0.5 ; K_R =5 ;T_R = 10;R = 2.4.

Transmission Line:

X_T = 0:16; X_L = 1.15; Xs=X_T+X_L=1.31.

Excitation system:

K_E = 50; T_E = 0.025.

Power System Stabilizer (PSS):

Ks = 2; Kw = 4; Tw = 4; T1= T3 = 2; T2= 0.638; T4= 0.824; T4= 0.06; Vsmax = 2; Vsmin = -2.

Heffron-philips model (HPM):

K1= 1.3907; K2= 1.0258; K3= 0.3597; K4= 1.3130; K5= -0.0337; K6= 0.5160.

Parameters of example Distributed energy resources(DER)

Gain constant (K):

K_{WTG1} = K_{WTG2} = 1.0; K_{AE} = 0.002; K_{PEMFC} = 0.01; K_{PV} = 1.0; K_{FESS} = -0.01; K_{BESS} = -0.003; K_{UC} = -0.7; K_{IDEG} = 0.003; K_{HVDC} = 0.005;

Time constants (T,s) :

T_{WTG1} = T_{WTG2} = 1.5; T_{AE} = 0.5; T_{PEMFC} = 4.0; T_{PV} = 1.8; T_{FESS} = 0.1; T_{BESS} = 0.9; T_{UC} = 0.9; T_{IDEG} = 2.0 ; T_{HVDC} = 0.7.

Appendix C.

Table 1A

1. Parameters to tune PI controllers for HPS-1

ENERGY STORAGE SYSTEMS	ELEMENTS	HVAC		HVDC	
		KP	KI	KP	KI
NO BESS-FESS	AE	-12.209	-7.82	-12.249	-0.213
	FC	6.05	-8.03	0.1	18.868
	IDEG	13.28	-0.013	9.497	12.120
BESS-FESS	AE	-22.8	6.36	-9.515	-0.121
	FC	0.38	-3.579	0.1	15.80
	IDEG	8.18	8.244	0.1	5.930
UC-FESS	AE	-15.27	-6.36	-8.541	-0.148
	FC	-0.99	4.93	12.643	3.237
	IDEG	1.93	1.68	7.608	6.970
HPM-BESS-FESS	AE	-12.209	-7.82	-9.515	-0.121
	FC	6.05	-8.03	12	-1.283
	IDEG	13.28	-0.013	0.1	5.937

2. Parameters to tune PI controllers for HPS-2

ENERGY STORAGE SYSTEMS	ELEMENTS	HVAC		HVDC	
		KP	KI	KP	KI
NO BESS-FESS	IDEG	17.28	0.50	12.820	0.0270
BESS-FESS	IDEG	25.98	0.349	4.767	0.270
UC-FESS	IDEG	15.89	6.94	0.220	2.490
HPM-BESS-FESS	IDEG	25.98	0.349	4.764	1.270

3. Parameters to tune PI controllers for HPS-3

ENERGY STORAGE SYSTEMS	ELEMENTS	HVAC		HVDC	
		KP	KI	KP	KI
NO BESS-FESS	AE	-18.20	-7.80	-5.27	-0.026
	FC	5.05	-5.02	16.26	0.56
	IDEG	10.28	-0.012	0.1	2.87

BESS-FESS	AE	-24.25	-1.30	-14.54	-0.2170
	FC	-24.20	0.055	0.1	39.740
	IDEG	0.05	5.20	0.1	14.416
UC-FESS	AE	-18.08	-4.60	-8.580	-0.1506
	FC	4.09	-0.232	12.752	3.315
	IDEG	8.130	2.082	7.590	7.075
HPM-BESS-FESS	AE	-24.25	-1.30	-9.515	-0.320
	FC	-24.25	0.055	14	-1.880
	IDEG	0.05	5.21	0.1	5.936

Appendix D. Quantitative analysis of S.I.E for different Hybrid Power Systems

Table 1B

1. Square Integral Error for different Hybrid Power Systems with HVAC line.

TOPOLOGIES	ENERGY SOURCES	HVAC	
		S.I.E without PI	S.I.E with PI
HPS-1	NO BESS-FESS	58.66	0.2401
	BESS-FESS	52.01	0.4003
	UC-FESS	3.12	0.0003642
	HPM-BESS-FESS	9.754e-06	9.956e-07
HPS-2	NO BESS-FESS	56.84	0.1147
	BESS-FESS	50.54	0.1458
HPS-2	UC-FESS	3.106	0.05994
	HPM-BESS-FESS	9.576e-06	9.664e-07
HPS-3	NO BESS-FESS	605.6	0.1
	BESS-FESS	536.4	0.1554
	UC-FESS	31.83	0.06451
	HPM-BESS-FESS	1.936e-06	1.645e-07

2. Square Integral Error for different Hybrid Power Systems with HVDC link.

TOPOLOGIES	ENERGY SOURCES	HVDC	
		S.I.E without PI	S.I.E with PI
HPS-1	NO BESS-FESS	141.3	0.03929
	BESS-FESS	52.1	0.07556
	UC-FESS	1.864	0.0223
	HPM-BESS-FESS	2.729e-06	2.488e-06
HPS-2	NO BESS-FESS	57.14	0.6562
HPS-2	BESS-FESS	50.8	0.2125
	UC-FESS	3.119	0.08953
	HPM-BESS-FESS	9.66e-06	3.372e-07
HPS-3	NO BESS-FESS	56.52	0.0549
	BESS-FESS	50.09	0.05281
	UC-FESS	3.473	0.02238
	HPM-BESS-FESS	0.0003668	9.812e-07

REFERENCES

[1] S.K Pandey, Soumya R. Mohanty, Nand Kishor.,''A literature survey on load- frequency control for conventional and distribution generation power systems," Energy Convers Manage 2013; 25:318-334.

[2] Power system stability and controlby Prabha kundur, Electrical power research institute, Tata Mcgrw Hill publications.

[3] JiaweiYanga, ZhuChea, ChengiongMao "Analysis and assessment of VSC excitation systemfor power system stability enhancement" Volume 57, May 2014, pp. 350-357.

[4] Debasish Mondal,Abhijit Chakrabarti,Aparajita Sengupta "Small-Signal Stability Analysis in SMIB Power System" May 2014.

[5] Bizon, Shayeghi, Nicu, Hossein, Mahdavi Tabatabaei, Naser.,"Analysis,control and optimal operations in hybrid power systems".

[6] S.K Pandey, Soumya R. Mohanty., ''Proportional integral controller based small signal analysis of hybrid

distributed generation system," Energy Convers Manage 2011; 52:1943–54.

[7] S.K.Pandey, Soumya R. Mohanty, ''Frequency regulation in hybrid power system using iterative proportional –integral–derivative H1 controller" Electric Power Compon Syst 2014; 42:132-48

[8] Md. Ibrahim, Abul Khair, Shaheer Ansari, Md. Ibrahim et al., ''A Review of hybrid renewable energy Systems for electric power generation" Int. Journal of Engineering Research and Applications 2002; 63: 9-26.

[9] Lakshmi Ravi, Vaidyanathan R, Shishir Kumar D, Prathika Appaiah, S.G. Bharathi Dasan,'' Optimal power flow with hybrid distributed generators and unified controller" TELKMONIKA Indonesian Journal of Electrical engineering. Vol.10, No.3, July 2012, pp.409~421.

[10] Paradkar A, Davari A, Feliachi A, Biswas T. "Integration of a fuel cell into the power system using an optimal controller based on disturbance accommodation control theory" J power Source, vol. 128, issue.2, pp.218-230, 2004.

[11] Modern power systems analysis by Kothari & nagrath, Tata Mcgrw Hill publications.

[12] Ochieng R. M, F. Onyango F. N and Oduor A. O, " Physical Formulation of the Expression of Wind Power", Internaltional Journal of Energy Environment and Economics, vol.18, pp.1-7,2010.

[13] Ahmed Nabil A, Miyatake Masafumi, Al-Othman AK. "Power fluctuations suppression of stand – alone hybrid generation combining solar photovoltaic

wind turbine and fuel cell systems", Vol.49 (10), Energy Convers Manage, April-2008.

[14] Gao W. "Performance comparison of a fuel cell-battery hybrid power train and a fuel cell-ultra capacitor hybrid power train, IEEE transactions on vehicular technology, Vol.54, No.3, May-2005

[15] Weissbach RS, Karady GG, Farmer RG. "Dynamic voltage compensation on distribution feeders using flywheel energy storage", IEEE Transactions on Power Delivery, Vol.14, No.2, April-1999

[16] Bresesti P,Kling WL,Hendriks RL,Vailati R."HVDC connection of offshore wind farms to the transmission system, IEEE transactions on Energy Conversion, Vol.22, No.1, March-2007

[17] Bhatti TS, Al-Ademi AAF, Bansal NK. "Load-frequency control of isolated wind diesel micro-hydro hybrid power systems", International Journal on Energy; Vol.22, No.5, pp.461–70, 1997.

[18] Abe Koji, Ohba Satoshi, Iwamoto S. "New load frequency control method suitable for large penetration of wind power generations", IEEE Conference Proc, pp.1–6, 2006.

[19] Lee DJ, Wang L. "Small-signal stability analysis of an autonomous hybrid renewableenergy power generation/energy storage system", part I: time domain Simulations. IEEE Transactions on Energy conversion, Vol. 23, No. 1, March-2008.

[20] Hoven Van der. "Power spectrum of horizontal wind speed in frequency range from 0.0007 to 900 cycles per hour", Journal of Meteorology, V0l.14, 1957.

[21] Nichita C, Luca D, Dakyo B, Ceanga E, Cutululis NA. "Modelling nonstationary wind speed for renewable energy systems", pp.289–94, SIMSIS 11, Galati. Romania, 2001.

[22] Anderson PM, Bose A. "Stability simulation of wind turbine system", IEEE Transactionson Power Apparatus and Systems, Vol. PAS-102, No. 12, December1983.

[23] Yu YN. "Electrical power system dynamics" .New York: Academica Press Inc.; 1983.

[24] Uzunollu M, Onar OC, Allam MS. Modeling, control and simulation of a PV/FC/UC based power generation system for stand-alone applications. Renew Energy 2008; 34 (3):509-20.

[25] Senjyuth – Nekajit – Uezatok - Fanabhashit: "A hybrid power systems using alternative energy facilities in isolated island", IEEE Trans. Energy Convers. 20 No. 2 (2005).